

1 **Atmospheric chemical processing dictates aerosol aluminum solubility: insights from**
2 **field measurement at two locations in northern China**

3

4 Tianyu Zhang,^{1,5} Yizhu Chen,^{1,5} Huanhuan Zhang,² Lei Liu,³ Chengpeng Huang,⁴ Zhengyang
5 Fang,^{1,a} Yifan Zhang,^{1,5} Fu Wang,⁴ Lan Luo,⁴ Guohua Zhang,¹ Xinming Wang,¹ Mingjin
6 Tang^{1,6,*}

7

8 ¹ State Key Laboratory of Advanced Environmental Technology and Guangdong Key
9 Laboratory of Environmental Protection and Resources Utilization, Guangzhou Institute
10 of Geochemistry, Chinese Academy of Sciences, Guangzhou, China

11 ² Guangzhou Marine Geological Survey, China Geological Survey, Guangzhou, China

12 ³ Hangzhou International Innovation Institute, Beihang University, Hangzhou, China

13 ⁴ Longhua Center for Disease Control and Prevention of Shenzhen, Shenzhen, China

14 ⁵ College of Earth and Planetary Sciences, University of Chinese Academy of Sciences, Beijing,
15 China

16 ⁶ Institute of Surface-Earth System Science, School of Earth System Science, Tianjin
17 University, Tianjin, China

18 ^a Current address: Institute of Low Temperature Science, Hokkaido University, Sapporo, 060-
19 0819, Japan

20 Correspondence: Mingjin Tang (mingjintang@126.com)

21

22

23 **Abstract**

24 Deposition of mineral dust aerosol into open oceans greatly impacts marine
25 biogeochemistry and primary production, and the deposition rates can be constrained using
26 dissolved aluminum (Al) in surface seawater as a tracer. However, aerosol Al solubility, a
27 critical parameter used in this method, remains highly uncertain. This work investigated
28 seasonal variations of aerosol Al solubility for supermicron and submicron particles at two
29 locations (Xi'an and Qingdao) in northern China. Aerosol Al solubility was found to be very
30 low at Xi'an and much higher at Qingdao. Furthermore, seasonal variability of Al solubility,
31 its correlation with relative abundance of sulfate and nitrate, and its dependence on relative
32 humidity, are all different at the two locations. We suggest that all the features observed for
33 aerosol Al solubility at the two locations can be well explained by the effects of atmospheric
34 chemical processing. Mineral dust transported to Xi'an (an inland city in Northwest China)
35 was still not obviously aged and thus chemical processing had little effects on aerosol Al
36 solubility. After arriving
37 g at Qingdao (a coastal city in the Northwest Pacific), mineral dust was substantially aged
38 by chemical processing, leading to substantial enhancement in aerosol Al solubility. Our work
39 further reveals that aerosol liquid water and acidity play vital roles in the dissolution of aerosol
40 Al by atmospheric chemical processing. We suggest that spatial variation of aerosol Al
41 solubility should be taken into account so that oceanic dust deposition can be better constrained
42 using dissolved Al concentrations in surface seawater.

43

44

45 **1. Introduction**

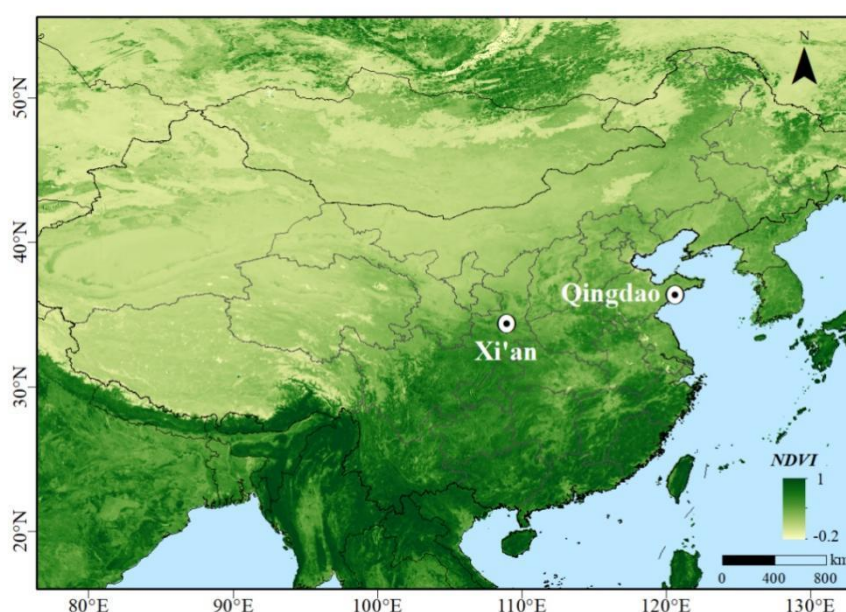
46 As an important type of tropospheric aerosols, mineral dust aerosol greatly impacts
47 atmosphere chemistry, climate, and ecological systems (Jickells et al., 2005; Tang et al., 2016;
48 Kok et al., 2023). After long-range transport, deposition of mineral dust into the oceans is a
49 major external source of several nutrient and toxic elements for surface seawater (Moore et al.,
50 2013; Westberry et al., 2023), impacting primary production and biogeochemical cycles in the
51 oceans and having further feedback on the climate system (Mahowald, 2011; Jiang et al., 2024).
52 The deposition flux of mineral dust aerosol into the oceans should be accurately estimated
53 before we can assess its impacts on marine biogeochemistry in a reliable manner (Schulz et al.,
54 2012; Anderson et al., 2016). Previous studies used several different methods to estimate dust
55 deposition fluxes and found large discrepancies (Huneeus et al., 2011; Anderson et al., 2016).

56 Deposition of mineral dust aerosol is the dominant source of dissolved aluminum (Al) in
57 the surface water of open oceans, and dissolved Al is generally considered to be chemically
58 and biologically inactive in seawater. As a result, dissolved Al concentrations in surface
59 seawater could be used to calculate dust deposition flux into the oceans (Measures and Brown,
60 1996; Measures and Vink, 2000), and the fractional solubility of aerosol Al (the fraction of
61 aerosol Al that can be dissolved) is one of the key parameters used in this method. Previous
62 studies which used this method to estimate dust depositions fluxes (Han et al., 2008; Measures
63 et al., 2010; Grand et al., 2015; Benaltabet et al., 2022) usually assumed uniform Al solubility
64 values in the range of 1.5-5%. However, field measurements found that aerosol Al solubility
65 could vary by more than an order of magnitude (Baker et al., 2006; Buck et al., 2013), and
66 thereby using a uniform aerosol Al solubility value could lead to large uncertainties in

67 estimated dust deposition fluxes (Han et al., 2008; Xu and Weber, 2021). As a result, it is
68 important to understand the spatiotemporal variations of aerosol Al solubility and elucidate the
69 processes and mechanisms which drive such variations.

70 The initial Al solubility is generally low (typically <1.5%) for dust particles over desert
71 regions (Shi et al., 2011; Aghnatiou et al., 2014; Li et al., 2022), and field studies found that
72 aerosol Al solubility in the troposphere could be much higher and showed wide variability. For
73 example, Al solubility ranged from 0.2-15.9% for total suspended particles (TSP) over the
74 Pacific (Buck et al., 2013), and were in the range of 3-78% over the Atlantic (Buck et al., 2010;
75 Chance et al., 2015). Some studies (Measures et al., 2010; Sakata et al., 2023) found good
76 correlations between dissolved aerosol Al (or Al solubility) and acid species in aerosol particles,
77 and thus suggested that chemical processes in the atmosphere could substantially enhance
78 aerosol Al solubility; furthermore, Li et al. (2017) found that Al solubility was remarkably
79 increased during cloud events when cloud processing enhanced the formation of secondary
80 inorganic ions (mainly sulfate and nitrate) and thus increased the acidity of cloud droplets.
81 However, Yang et al. (2023) found no correlations between Al solubility and the concentrations
82 of aerosol acidic species, and concluded that the effect of acid processing on Al solubility was
83 negligible. Aerosol Al solubility over the Atlantic appeared to be higher for air masses from
84 Europe than those from the Saharan region (Baker et al., 2006; López-García et al., 2017), and
85 some studies hypothesized that this could be potentially explained by the influence of
86 anthropogenic aerosol Al if it had higher solubility than mineral dust (Paris et al., 2010; López-
87 García et al., 2017).

88 It can be concluded that although aerosol Al solubility in the atmosphere was explored by
89 several previous studies, our understanding is still very limited. For example, it remains unclear
90 why aerosol Al solubility shows large spatial and temporal variation. Some work suggested
91 that atmospheric chemical aging could enhance aerosol Al solubility, but the mechanisms and
92 key environmental factors have not been elucidated. Furthermore, the effects of particle size
93 on aerosol Al solubility have not been well understood.



94
95 **Figure 1.** A map of East Asia and surrounding areas. The two locations (Xi'an and Qingdao)
96 where we collected aerosol particles are highlighted. NDVI: normalized difference vegetation
97 index provided by MODIS (Moderate Resolution Imaging Spectroradiometer).

98
99 In this work, we collected supermicron ($>1 \mu\text{m}$) and submicron ($<1 \mu\text{m}$) aerosol particles
100 at Xi'an and Qingdao, both located in northern China, and investigated seasonal variations of
101 aerosol Al solubility at these two locations. Taklimakan and Gobi Deserts in northwestern
102 China are two important source regions of Asian dust (Prospero et al., 2002). As shown in

103 Figure 1, Xi'an is an inland city in northwestern China, and the aging extent of dust was found
104 to be quite limited at Xi'an due to its proximity of desert regions (Wang et al., 2014; Wu et al.,
105 2017). As Asian dust is transported eastward, it passes over the North China Plain where
106 anthropogenic emission is very high, and may become much more aged when arriving at
107 Qingdao, a coastal city of the Northwest Pacific (Li et al., 2014; Pan et al., 2017). By comparing
108 aerosol Al solubility at Xi'an and Qingdao, our work can provide valuable insights into how
109 and to which extent aging processes during long-range transport can change aerosol Al
110 solubility. Dust aerosol concentrations and meteorological conditions vary remarkably at
111 different seasons in Northern China; as a result, examining its seasonal variations provides a
112 good opportunity to understand the factors which regulate aerosol Al solubility.

113 **2. Materials and methods**

114 **2.1 Sample collection**

115 Samples were collected at two cities (Xi'an and Qingdao) in northern China at four
116 different seasons during 2021-2023 (Zhang et al., 2023; Chen et al., 2024), and further details
117 can be found in the supplement (Text S1 and Table S1). In brief, supermicron ($>1\ \mu\text{m}$) and
118 submicron ($<1\ \mu\text{m}$) particles were simultaneously collected using a two-stage aerosol sampler
119 (TH-150C, Tianhong Co., China) which was operated at 100 L/min, and the sampling duration
120 was typically 23.5 hours for each pair of aerosol samples. Whatman 41 cellulose filters were
121 used for aerosol collection in our work, and they were acid-washed before being used for
122 aerosol sampling to reduce background levels (Zhang et al., 2022). A total of 126 and 106 pairs
123 of aerosol samples were collected at Xi'an and Qingdao, respectively (Zhang et al., 2023; Chen
124 et al., 2024). After collection, all the aerosol samples were stored at -20°C for further analysis.

125 In addition to aerosol particles, we also sampled atmospheric acidic and alkaline gases
126 (mainly NH_3 , HCl and HNO_3) at Qingdao, using a ChemComb 3500 Speciation Collection
127 Cartridge (Thermo Fisher Scientific, USA) at a flow rate of 10 L/min (Walters and Hastings,
128 2018; Fang et al., 2025). Gas sampling was carried out concurrently with aerosol sampling. In
129 brief, NH_3 , HNO_3 and HCl were absorbed onto the inner walls of two tandem honeycomb
130 diffusion tubes coated with proper adsorbents, and then converted into NH_4^+ , NO_3^- and Cl^- .
131 After the sampling was completed, 20 mL ultrapure water was used to rinse each tube
132 immediately, and a PTFE membrane syringe filter (0.22 μm in pore size) was used to filter the
133 solution. The solution was then frozen at -20°C for further analysis.

134 **2.2 Sample analysis and aerosol acidity calculation**

135 Sample pretreatment and analysis were detailed in our previous work (Zhang et al., 2022),
136 and therefore are only briefly summarized here. The first half of a filter (and only one quarter
137 of a filter for supermicron particles) was shredded and digested in a Teflon jar using a
138 microwave digestion instrument. After digestion, the Teflon jar was filled with 1% HNO_3 (20
139 mL), and a PTFE membrane syringe filter (0.22 μm in pore size) was used to filter the solution;
140 subsequently, the solution was analyzed by inductively coupled plasma-mass spectrometry
141 (ICP-MS) to determine total concentrations of individual trace elements, including Al.

142 The other half of a filter was immersed in ultrapure water (20 mL) and stirred using an
143 orbital shaking for two hours; in the next step, the solution was filtered using a PTFE membrane
144 syringe filter (0.22 μm in pore size) and divided into two parts. The first solution was acidified
145 to contain 1% HNO_3 and subsequently analyzed by ICP-MS to determine the concentrations
146 of dissolved trace elements; the second solution was analyzed by ion chromatography (IC) to

147 quantify the concentration of water-soluble cations and anions.

148 The solutions obtained from honeycomb diffusion tubes (see Section 2.1 for more details)
149 were also analyzed using IC to determine the concentrations of gaseous NH_3 , HCl and HNO_3
150 in the atmosphere. ISORROPIA-II, a widely used aerosol thermodynamic model (Fountoukis
151 and Nenes, 2007), was employed in this work to calculate the acidity of supermicron and
152 submicron particles. It was operated in the forward mode, and aerosol particles were assumed
153 to remain metastable. Input parameters included concentrations of water-soluble ions in aerosol
154 particles and gaseous NH_3 , HCl and HNO_3 , temperature and relative humidity (RH). Our
155 previous work found good agreement between measured and calculated NH_3 partitioning
156 coefficients at Qingdao (Fang et al., 2025), and as a result the method we used could well
157 estimate the acidity of supermicron and submicron particles.

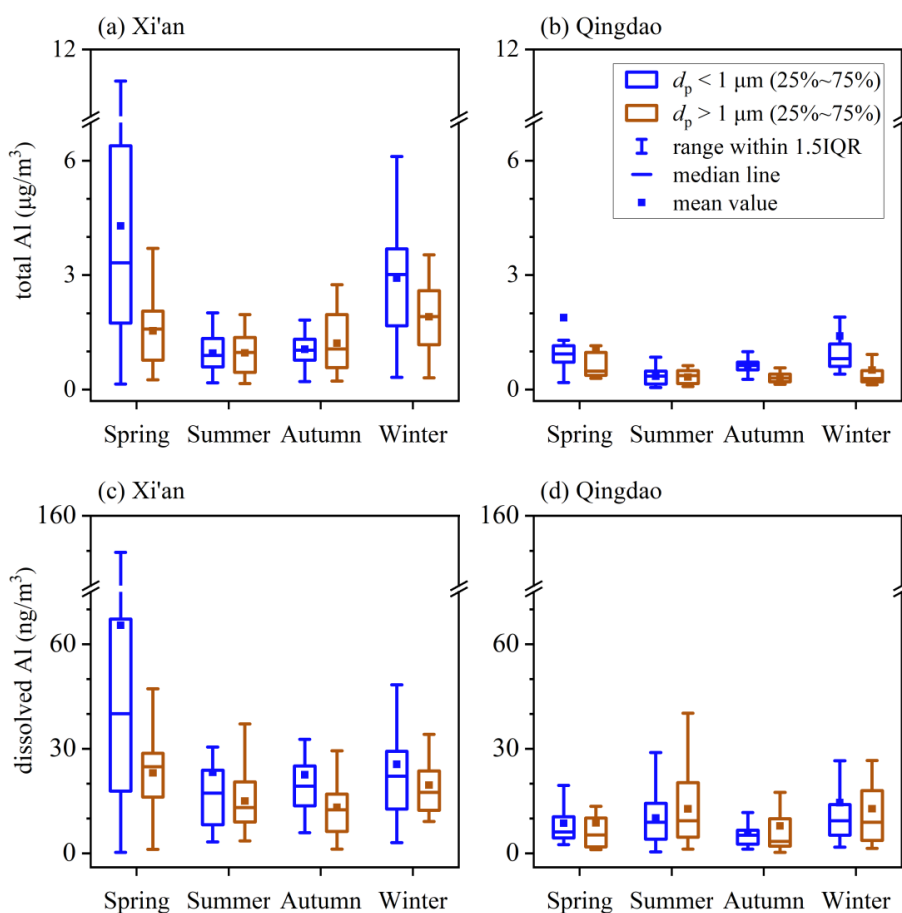
158 **3. Results**

159 **3.1 Seasonal variations of total and dissolved aerosol Al**

160 **3.1.1 Total aerosol Al**

161 Figure 2 displays seasonal variations of total and dissolved aerosol Al at Xi'an and
162 Qingdao. At Xi'an (Figure 2a), total Al in supermicron particles showed highest concentrations
163 in spring and winter (1.54 ± 0.89 and $1.91 \pm 0.93 \mu\text{g}/\text{m}^3$) and lowest concentrations in summer
164 ($0.96 \pm 0.54 \mu\text{g}/\text{m}^3$); a similar seasonal pattern was observed for submicron particles, with total
165 Al concentrations being highest in spring and winter (4.29 ± 3.70 and $2.92 \pm 1.47 \mu\text{g}/\text{m}^3$) and
166 lowest in summer ($0.95 \pm 0.44 \mu\text{g}/\text{m}^3$). At Qingdao (Figure 2b), total Al concentrations in
167 supermicron particles were highest in spring ($1.04 \pm 1.12 \mu\text{g}/\text{m}^3$) and lowest in summer and
168 autumn (0.33 ± 0.18 and $0.31 \pm 0.12 \mu\text{g}/\text{m}^3$); similarly, for submicron particles, total Al

169 concentrations were also highest in spring ($1.88 \pm 2.51 \mu\text{g}/\text{m}^3$) and lowest in summer and
 170 autumn (0.35 ± 0.22 and $0.65 \pm 0.82 \mu\text{g}/\text{m}^3$). For each season the median concentration of total
 171 aerosol Al was usually higher in submicron particles than supermicron particles at both
 172 locations (and there were some exceptions, as shown in Figures 1a and 1b). This is related to
 173 size dependence of mineralogy and elemental compositions of mineral dust aerosol, which is
 174 not well studied and deserves further investigation.



175
 176 **Figure 2.** Seasonal variations of total and dissolved aerosol Al for submicron and supermicron
 177 particles: (a) total Al at Xi'an; (b) total Al at Qingdao; (c) dissolved Al at Xi'an; (d) dissolved
 178 Al at Qingdao.

179
 180 Overall, total aerosol Al concentrations showed similar seasonal variations at Xi'an and

181 Qingdao, being highest in spring and lowest in summer. This was consistent with previous
182 studies carried out in other locations in East Asia, such as Zhengzhou (Wang et al., 2019),
183 Beijing (Zhang et al., 2013), Huaniao Island in the East China Sea (Guo et al., 2014), and Japan
184 (Sakata et al., 2023). In East Asia, mineral dust aerosol was emitted into the atmosphere mainly
185 in spring, leading to the increase in total aerosol Al concentrations. Lowest concentrations of
186 total aerosol Al were observed in summer because precipitation in Northern China mainly
187 occurred in summer, leading to enhanced wet deposition of aerosol particles (Cao and Cui,
188 2021). Furthermore, Qingdao was frequently affected by marine air masses in summer, and
189 this is also one reason why total aerosol Al concentrations were lower in summer than other
190 seasons. Total aerosol Al concentrations were higher in winter than summer and autumn at
191 Xi'an, and one major reason is that meteorological conditions favored the accumulation of
192 aerosol particles (including aerosol Al) during winter (Cao and Cui, 2021).

193 As summarized in the supplement (Table S2), total aerosol Al concentrations exhibited
194 evident spatial variations in East Asia. As Asian dust was transported eastward to the North
195 Pacific, a clear decrease in aerosol Al concentrations was observed. Mineral dust was the
196 dominant source for aerosol Al, and therefore concentrations of aerosol Al were found to be
197 very high in desert regions. For example, total Al concentrations in TSP could reach $24 \mu\text{g}/\text{m}^3$
198 over the Taklimakan Desert (Zhang et al., 2003). In our current study, annual average total Al
199 concentrations at Xi'an, an inland city close to the desert, were reported to be 1.42 ± 0.86 and
200 $2.28 \pm 2.35 \mu\text{g}/\text{m}^3$ for supermicron and submicron particles, much lower than that observed over
201 the Taklimakan Desert. Further decrease in total Al concentrations was observed in coastal and
202 oceanic regions. For example, our work found that the annual average total Al concentrations

203 were 0.56 ± 0.75 and 1.08 ± 1.67 $\mu\text{g}/\text{m}^3$ for supermicron and submicron particles at Qingdao,
204 lower than those at Xi'an; total Al concentrations in TSP ranged from 0.17 to 1.72 $\mu\text{g}/\text{m}^3$ in
205 Hiroshima (Sakata et al., 2023), and further decreased to 1-56 ng/m^3 in Hawaii in the central
206 Pacific (Measures et al., 2010).

207 3.1.2 Dissolved aerosol Al

208 At Xi'an (Figure 2c), for supermicron particles, dissolved aerosol Al concentrations were
209 highest in spring (23.1 ± 10.9 ng/m^3) and lowest in summer and autumn (15.0 ± 8.7 and 13.2 ± 8.6
210 ng/m^3); for submicron particles, dissolved Al concentrations were also highest in spring
211 (65.4 ± 79.2 ng/m^3) and lowest in summer and autumn (23.2 ± 23.4 and 22.6 ± 20.1 ng/m^3). Total
212 (Figure 2a) and dissolved aerosol Al (Figure 2c) showed similar seasonal patterns at Xi'an,
213 indicating that dissolved aerosol Al was mainly regulated by total aerosol Al.

214 As shown in Figure 2d, the average dissolved aerosol Al concentrations were 8.8 ± 10.8 ,
215 12.8 ± 11.1 , 7.9 ± 10.5 and 12.8 ± 12.9 ng/m^3 for supermicron particles at Qingdao in spring,
216 summer, autumn, and winter, respectively, and 8.7 ± 5.8 , 10.2 ± 8.2 , 6.0 ± 4.8 and 14.5 ± 15.2 ng/m^3
217 for submicron particles. Dissolved aerosol Al concentrations were highest in summer and
218 winter and lowest in autumn for both supermicron and submicron particles. In contrast to Xi'an,
219 total and dissolved aerosol Al at Qingdao showed different seasonal patterns (Figures 2b and
220 2d); for example, total Al concentrations were lowest in summer at Qingdao when dissolved
221 Al concentrations were highest. This indicates that dissolved aerosol Al at Qingdao was not
222 only regulated by total aerosol Al but also affected by other factors such as atmospheric aging
223 processes.

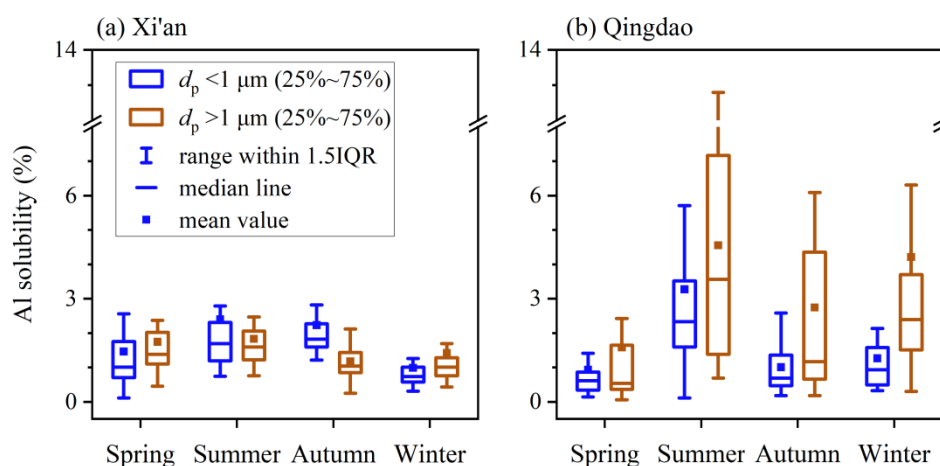
224 Compared to Xi'an, dissolved Al concentrations at Qingdao were lower across all the four

225 seasons, mainly because total Al concentrations were much lower at Qingdao (Tables S3-S4 in
 226 the supplement). As shown in Figure 2, similar seasonal patterns were observed at two
 227 locations for total aerosol Al, but dissolved aerosol Al showed very different seasonality; this
 228 suggests that seasonal patterns of aerosol Al solubility were different at Xi'an and Qingdao, as
 229 presented in Section 3.2.

230 3.2 Fractional solubility of aerosol Al

231 3.2.1 Seasonal variations of Al solubility

232 Figure 3 displays aerosol Al solubility in different seasons at Xi'an and Qingdao. The
 233 median solubilities of aerosol Al were determined to be 1.38%, 1.59%, 1.04% and 1.01% for
 234 supermicron particles at Xi'an in spring, summer, autumn and winter, respectively, and 1.01%,
 235 1.69%, 1.82% and 0.74% for submicron particles. Aerosol Al solubilities were generally low
 236 for the four seasons at Xi'an, showing no apparent variation with seasons (Figure 3a). In
 237 contrast, aerosol Al solubilities exhibited distinct seasonal variability at Qingdao (Figure 3b),
 238 and the median Al solubilities were highest in summer (3.56% and 2.33%) and lowest in spring
 239 (0.54% and 0.61%) for both supermicron and submicron particles.



240

241 **Figure 3.** Seasonal variations of aerosol Al solubility for submicron and supermicron particles

242 at (a) Xi'an and (b) Qingdao.

243

244 In three seasons (summer, autumn and winter), aerosol Al solubility at Qingdao was
245 higher than that at Xi'an (Figure 3, Table S5). There are several important dust sources in
246 Northwest China, being far from (up to a few thousand km) or close to Xi'an. More importantly,
247 anthropogenic emission in Northwest China is much smaller than the North China Plain, and
248 thus the aging extent of mineral dust transported to Xi'an was rather limited (Wang et al., 2014;
249 Wu et al., 2017). On the contrary, Qingdao is much farther from deserts; consequently, after
250 long-distance transport over the North China Plain where anthropogenic emission is very large,
251 mineral dust aerosol which arrived at Qingdao was substantially aged (Trochkin et al., 2003;
252 Takahashi et al., 2011; Jeong, 2020), thereby leading to enhanced dissolution of aerosol Al and
253 thus the increase in Al solubility. Mineral dust from different desert regions and local
254 suspended dust cannot explain higher Al aerosol solubility observed at Qingdao, as previous
255 work showed that Al solubility was low for soil samples from different regions (Shi et al., 2011;
256 Wuttig et al., 2013; Aghnatiou et al., 2014; Li et al., 2022; Hsieh et al., 2023).

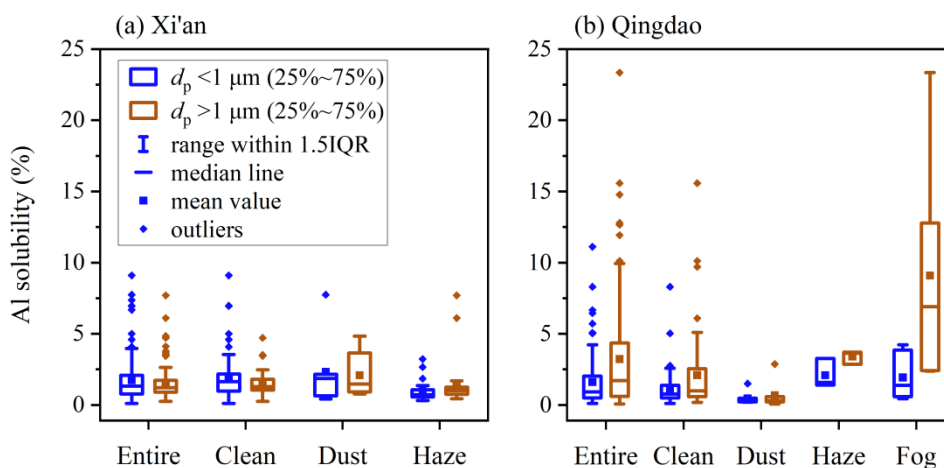
257 On the other hand, no obvious difference in aerosol Al solubility was observed between
258 Xi'an and Qingdao in spring, with median aerosol Al solubilities being <1.4% for supermicron
259 and submicron particles (Figure 3). This agrees with a previous study (Hsu et al., 2010) which
260 found that aerosol Al solubility was very low (average: ~0.7%) in spring even over the East
261 China Sea. Furthermore, similar to what we observed in spring at Xi'an and Qingdao, Al
262 solubility was found to be low (<1.5%) for surface soil particles collected from deserts (Shi et
263 al., 2011; Aghnatiou et al., 2014; Li et al., 2022). Overall, our work implies that in spring when

264 Asian dust occurred most frequently, mineral dust particles arriving at Qingdao after long-
265 distance transport did not show substantial increase in Al solubility.

266 **3.2.2 Al solubility under different weather conditions**

267 We encountered four representative weather conditions (i.e. clean, dust, haze and fog days)
268 during our sampling at Xi'an and Qingdao, and investigated aerosol Al solubility under
269 different weather conditions (Figure 4, Tables S6-S7).

270 At Xi'an, no apparent difference in Al solubility was observed during clean, haze, and
271 dust days (Figure 4a, Table S6), with median values in the range of 1.01-1.47% for supermicron
272 particles and 0.72-1.86% for submicron particles. Al solubility was found to be <1.2% for three
273 mineral dust samples (Luochuan loess, Arizona test dust, and dust collected during a dust storm
274 in Xinjiang) (Li et al., 2022), and ranged from 0.47% to 1.42% for aerosol particles generated
275 using soil samples from Saharan desert (Shi et al., 2011). Compared to mineral dust in source
276 regions, Al solubility was not higher under different weather conditions at Xi'an. In addition,
277 although emission and accumulation of anthropogenic pollutants was greatly enhanced during
278 haze days at Xi'an (An et al., 2019; Cao and Cui, 2021), there was no obvious increase in
279 aerosol Al solubility, indicating that the effects of anthropogenic emissions on aerosol Al
280 solubility was limited at Xi'an. Therefore, one may conclude that aerosol Al solubility at Xi'an
281 was not different from initial Al solubility of mineral dust.



282

283 **Figure 4.** Aerosol Al solubility under different weather conditions for submicron and
 284 supermicron particles: (a) Xi'an, (b) Qingdao.

285

286 Being different to Xi'an, aerosol Al solubility at Qingdao shows remarkable variations
 287 under different weather conditions (Figure 4b, Table S7). Median Al solubilities were
 288 determined to be 0.31% and 0.24% for supermicron and submicron particles during dust days,
 289 lower than these on clean days (0.99% and 0.77%, respectively). This is probably because
 290 higher wind speeds during dust events hindered the accumulation of atmospheric pollutants
 291 and shortened the transport time to Qingdao, and thus limiting the aging of mineral dust aerosol.
 292 This explanation is supported by a recent study (Zhang et al., 2024) which found that the aging
 293 extent of dust particles in Japan was much lower during fast-moving dust events than slow-
 294 moving dust events. Moreover, large amounts of alkaline components (such as carbonates)
 295 which were emitted to the atmosphere during dust days neutralized acid species and therefore
 296 inhibited acid-promoted dissolution of aerosol trace elements (Zhi et al., 2025).

297 Figure 4b also suggests that aerosol Al solubilities were much higher during haze and fog
 298 days at Qingdao, when compared to clean days. Highest Al solubilities were observed during

299 fog days, with median values being 6.90% for supermicron particles and 1.38% for submicron
300 particles, followed by haze days (3.64% and 1.58%, respectively). This is very likely due to
301 enhanced chemical processing during haze and fog periods (Shi et al., 2020; Shang et al., 2024),
302 and especially during fog days the large increase in RH cause huge increase in aerosol liquid
303 water, therefore greatly promoting aqueous reactions and Al dissolution. Acid and ligand
304 processing can both enhance aerosol Al solubility, although at present it is difficult to
305 disentangle their individual contributions.

306 In summary, aerosol Al solubility at Xi'an was low in general, and did not show much
307 variability in different seasons or under different weather conditions. Compared to Xi'an,
308 aerosol Al solubility was higher at Qingdao; furthermore, it was higher in the other three
309 seasons than in spring, and much higher for haze and fog days than dust days. These results
310 imply that atmospheric aging had little effects on aerosol Al solubility at Xi'an but could
311 remarkably increase aerosol Al solubility at Qingdao, as further elaborated in Section 4.

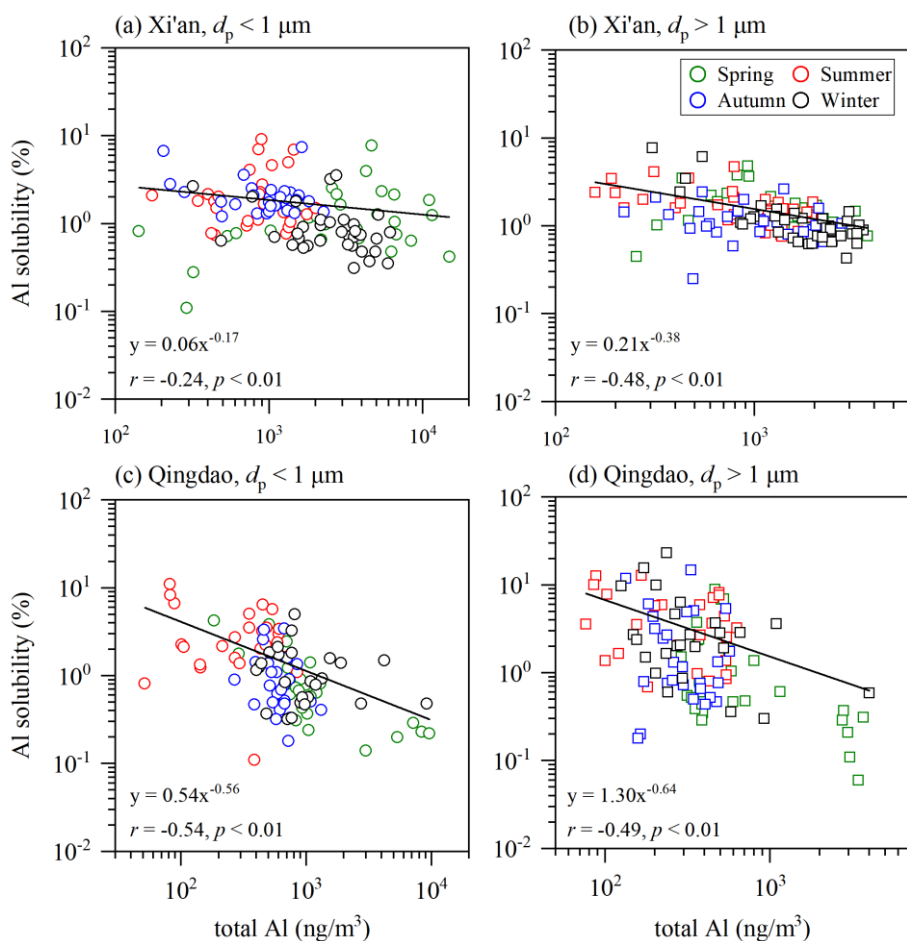
312 **4. Discussion**

313 As shown in Figure 5, our work observed the inverse dependence of aerosol Al solubility
314 on total Al concentrations at both Xi'an and Qingdao, given by Eq. (1):

$$315 \quad f_s(\text{Al}) = a \times [\text{Al}]^{-b} \quad (1)$$

316 where $f_s(\text{Al})$ is aerosol Al solubility (%) and $[\text{Al}]$ is total Al concentration (ng/m^3). Such
317 relationship was also reported in some previous studies (Jickells et al., 2016; Shelley et al.,
318 2018; Baker et al., 2020; Shelley et al., 2025). Baker and Jickells (2006) suggested that such
319 inverse relationship was due to that larger particles have higher deposition velocities and lower
320 Al solubility: aerosol Al concentrations decrease during transport in the atmosphere due to

321 deposition, with deposition being faster for larger particles; as a result, aerosol particles will be
 322 enriched with smaller particles with higher Al solubility. However, Shi et al. (2011) found no
 323 substantial change in Al solubility with particle size for mineral dust samples, and therefore
 324 put the explanation proposed by Baker and Jickells (2006) into doubt.



325
 326 **Figure 5.** Aerosol Al solubility versus total aerosol Al concentrations: (a) submicron particles
 327 at Xi'an, (b) supermicron particles at Xi'an, (c) submicron particles at Qingdao, (d)
 328 supermicron particles at Qingdao.

329
 330 Aerosol Fe solubility was also frequently observed to increase with the decrease in total
 331 Fe concentrations (Sedwick et al., 2007; Mahowald et al., 2018; Meskhidze et al., 2019), and

332 one possible reason is the influence of anthropogenic aerosol Fe (Sholkovitz et al., 2009; Ito
333 and Shi, 2016) with higher solubility than mineral dust (Schroth et al., 2009; Fu et al., 2012;
334 Ito et al., 2021). Nevertheless, being different from aerosol Fe, aerosol Al stems predominantly
335 from mineral dust, with little contribution from anthropogenic sources; furthermore, Al
336 solubility was measured to be $0.4\pm 0.6\%$ for coal fly ash (Li et al., 2022), an important type of
337 anthropogenic aerosols, not higher than that for mineral dust ($0.8\pm 0.4\%$). Therefore, we suggest
338 that anthropogenic emission may not be able to explain the inverse dependence of Al aerosol
339 solubility on total Al concentrations.

340 We argue that chemical processing in the atmosphere can very well explain such inverse
341 dependence. Total aerosol Al concentrations decrease with transport due to deposition, while
342 reactions with acidic gases (such as SO_2 and NO_x) can enhance the dissolution of aerosol Al
343 (Jickells et al., 2016). Figure 5 shows that the inverse dependence of Al solubility on total Al
344 concentration was more pronounced at Qingdao, with the slopes (b values) much larger than
345 those obtained at Xi'an. This is because compared to Xi'an, Qingdao is more distant from
346 deserts and therefore dust aerosol is expected to be more aged at Qingdao. It also further
347 supports the vital role chemical aging plays in regulating aerosol Al solubility,

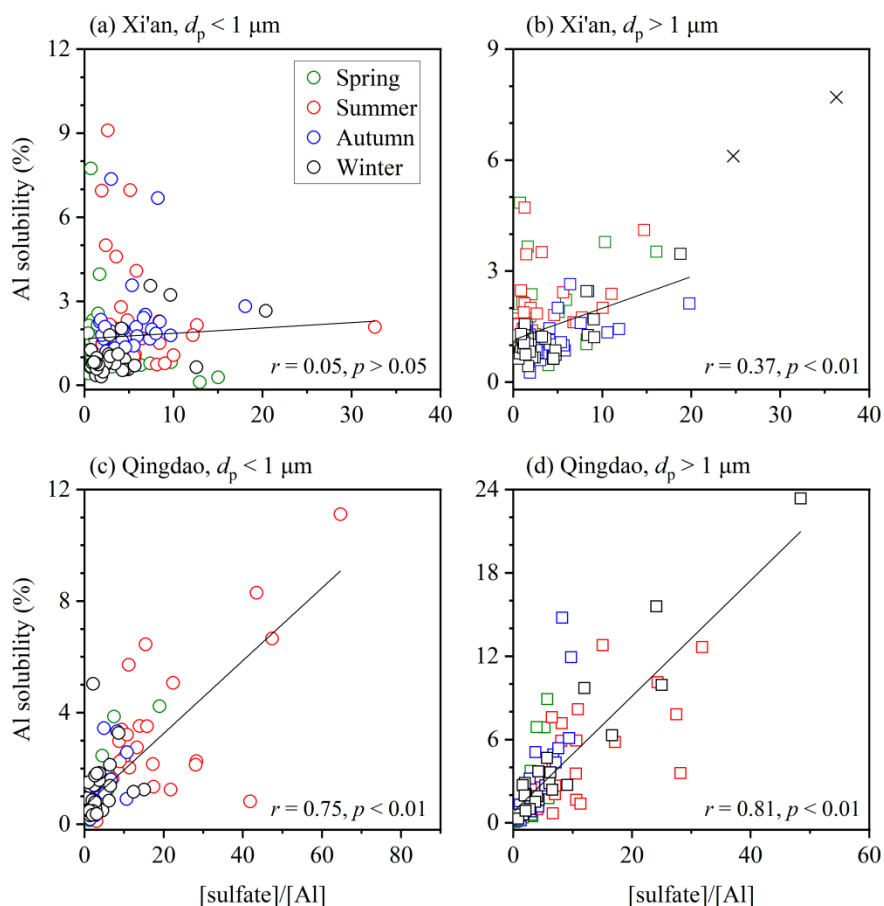
348 **4.1 Effects of acid processing and the role of RH**

349 **4.1.1 Effects of acid processing**

350 Laboratory experiments found that the amount of Al dissolved from minerals would
351 increase with the decrease in solution pH (Amram and Ganor, 2005; Bibi et al., 2011, 2014;
352 Cappelli et al., 2018), and some field measurements also suggested that acid processing in the
353 atmosphere could lead to large increase in aerosol Al solubility (Measures et al., 2010; Sakata

354 et al., 2023). In this work, we examined the relationship between aerosol Al solubility and the
355 relative abundance of acidic species ($[\text{sulfate}]/[\text{Al}]$ and $[\text{nitrate}]/[\text{Al}]$) at Xi'an and Qingdao. It
356 should be noted that non-sea-salts sulfate (Virkkula et al., 2006), instead of sulfate, was used
357 at Qingdao because it is a coastal city and heavily impacted by sea spray aerosol.

358 At Xi'an, overall aerosol Al solubility showed no significant correlation with $[\text{sulfate}]/[\text{Al}]$
359 or $[\text{nitrate}]/[\text{Al}]$ for either supermicron or submicron particles ($r < 0.4$, Figure 6 and S1),
360 indicating that acid processing did not enhance aerosol Al solubility. Enhancement of aerosol
361 trace element solubility by acid processing requires internal mixing of acid species with mineral
362 dust particles (Baker and Croot, 2010). Previous studies suggested that mineral dust particles
363 observed at Xi'an which is close to deserts largely remained externally mixed with acid species
364 (Wang et al., 2014; Wu et al., 2017), and thus aerosol Al solubility was not apparently enhanced
365 by acid processing at Xi'an.



366

367 **Figure 6.** Aerosol Al solubility versus [sulfate]/[Al]: (a) submicron particles at Xi'an, (b)
 368 supermicron particles at Xi'an, (c) submicron particles at Qingdao, (d) supermicron particles
 369 at Qingdao. Data represented by crosses are not included in fitting.

370

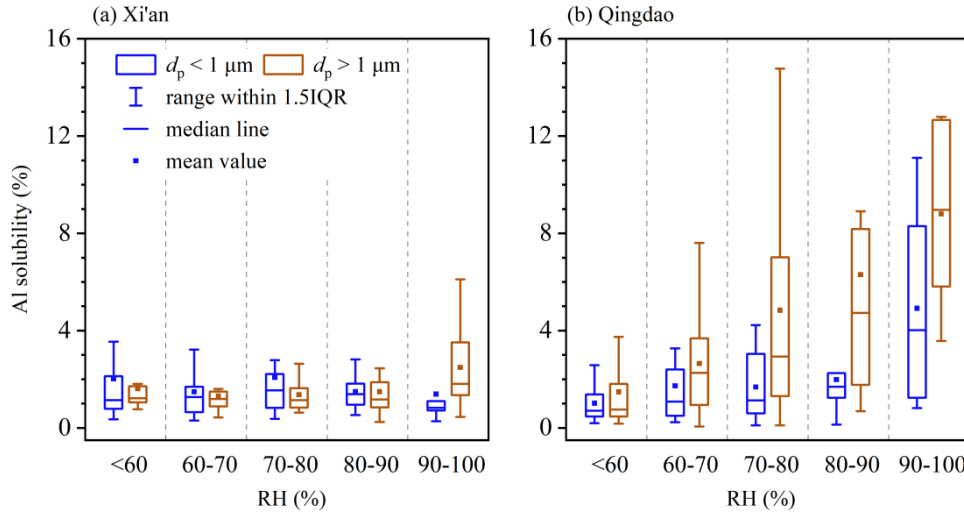
371 On the contrary, Figure 6 shows that aerosol Al solubility at Qingdao was well correlated
 372 with [sulfate]/[Al] ($r > 0.7, p < 0.01$), implying that acid-promoted dissolution significantly
 373 enhanced Al solubility. We also found that correlations of Al solubility with [sulfate]/[Al] was
 374 better than those with [nitrate]/[Al] (Figures 6 and S1, Table S8), in line with a previous study
 375 (Sakata et al., 2023) which found aerosol Al solubility at Hiroshima, southern Japan, to be
 376 correlated with [sulfate]/[Al] but not with [nitrate]/[Al]. This may imply that chemical

377 processing by sulfate was more important than nitrate for Al solubility enhancement via acid
378 processing, likely because aluminosilicate dust particles tend to react preferentially with SO₂
379 and H₂SO₄ while nitrogen oxides react mainly with carbonate particles (Sullivan et al., 2007;
380 Fitzgerald et al., 2015). Furthermore, our work reveals better correlations between Al solubility
381 and [sulfate]/[Al] for supermicron particles than submicron particles (Figure 6), indicating that
382 the effect of acid processing on Al solubility was more important in supermicron particles.

383 **4.1.2 The role of RH**

384 Relative humidity (RH) is a vital factor influencing liquid water contents and phase state
385 of aerosol particles and thus their secondary chemistry. When RH increased >60%, the phase
386 state of aerosol particles in northern China changed from semisolid to liquid (Liu et al., 2017;
387 Sun et al., 2018; Song et al., 2022), leading to large increase in aerosol liquid water content and
388 thereby potentially affecting aerosol Al solubility.

389 We observed no apparent variation of aerosol Al solubility with RH at Xi'an (Figure 7a).
390 When RH was <60%, median Al solubilities for supermicron and submicron particles were
391 1.22% and 1.14%, respectively; when RH increased >90%, the median Al solubilities were
392 determined to be 1.82% and 0.82%, showing no obvious increase when compared to those at
393 <60% RH. This again may imply that chemical processing had very limited impact on aerosol
394 Al solubility at Xi'an, as mineral dust particles mostly remained externally mixed with
395 secondary species and their aging extent was very limited (Wang et al., 2014; Wu et al., 2017).



396

397 **Figure 7.** Aerosol Al solubility at different relative humidity (RH) for submicron and
 398 supermicron particles: (a) Xi'an, (b) Qingdao.

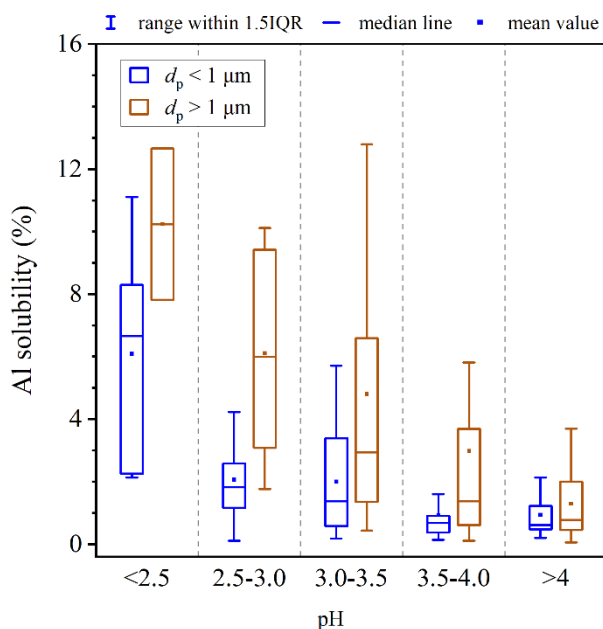
399

400 In contrast, RH played an important role in regulating aerosol Al solubility at Qingdao,
 401 because mineral dust particles observed at Qingdao had been transported through the North
 402 China Plain and were substantially aged. As shown in Figure 7b, for supermicron particles, the
 403 median Al solubility was only 0.76% at <60% RH, and gradually increased to 4.73% at 80-90%
 404 RH, and abruptly increased to 8.87% at >90% RH. For submicron particles, median Al
 405 solubility was <1% at <60% RH, and further increase in RH to 80-90% did not lead to large
 406 changes in Al solubility; nevertheless, when RH exceeded 90%, the median Al solubility was
 407 remarkably increased to 4.02%, much higher than those observed when RH was < 90%.

408 4.2 Effects of aerosol acidity on aerosol Al solubility at Qingdao

409 Figure 8 shows the dependence of aerosol Al solubility on aerosol acidity (represented by
 410 pH) at Qingdao (we did not measure NH_3 at Xi'an and thus could not estimate the aerosol
 411 acidity in a reliable manner). For supermicron particles, the median Al solubility was only 0.99%

412 when aerosol pH was >4.0 , and gradually increased to 10.24% as aerosol pH was decreased to
 413 <2.5 . For submicron particles, the median Al solubility was only 0.69% when pH was >4.0 ,
 414 increased slightly with the decrease in pH when pH was in the range of 2.5-4.0, and then
 415 increased greatly to 6.09% when pH was decreased to <2.5 . In addition, aerosol acidity at
 416 Qingdao was highest in summer and lowest in spring (Chen et al., 2024), consistent with the
 417 seasonal variation of aerosol Al solubility, further supporting the importance of aerosol acidity
 418 in regulating Al solubility.



419
 420 **Figure 8.** Aerosol Al solubility corresponding to different aerosol acidity for submicron and
 421 supermicron particles in Qingdao.

422
 423 As shown in Figure S2, aerosol Al solubility was generally $<2\%$ when aerosol acidity was
 424 low (pH >4.0), and higher Al solubility ($>2\%$) was usually observed for samples with high RH
 425 and high acidity (pH <4.0), again underscoring the roles of aerosol acidity (and RH). However,
 426 some samples exhibited low Al solubility although the corresponding RH and aerosol acidity

427 were both higher, and such phenomenon was more pronounced for submicron particles. This
428 is very likely linked with aerosol mixing state (Riemer et al., 2019). Aerosol Al solubility and
429 acidity used in our work are both the average properties of an aerosol sample which contains
430 numerous particles, while in reality the two properties will have large particle-to-particle
431 variations. For a given aerosol sample, it can happen that particles with high acidity may
432 contain very little Al while particles with low acidity are enriched in Al; in this case, high
433 acidity do not promote Al solubility for this sample. Single particle analysis which provides
434 mixing state information can give further insights. We also note that samples with low Al
435 solubility but high RH and high acidity were mostly found in clean days, perhaps due to the
436 influence of local resuspended dust for which chemical aging was very limited.

437 **4.3 Size-dependence of aerosol Al solubility**

438 At Xi'an, no obvious difference in aerosol Al solubility was found between supermicron
439 and submicron particles across all the four seasons (Figure 3a). This is because the aging extent
440 of dust particles was rather limited at Xi'an (Wang et al., 2014; Wu et al., 2017) and Al
441 solubility does not vary with particle size for unaged dust particles (Shi et al., 2011). At
442 Qingdao, aerosol Al solubility showed no obvious difference between supermicron and
443 submicron particles in spring, because the aging extent of dust arriving at Qingdao was also
444 limited in spring when Asian dust occurred most frequently. However, in the other three
445 seasons, Al solubility was higher for supermicron particles than submicron particles at Qingdao,
446 and the ratios of median Al solubility in supermicron particles to that in submicron particles
447 were found to be 1.53, 1.70 and 2.57 in summer, autumn and winter, respectively. Similar to

448 our observation at Qingdao, Li et al. (2017) found that aerosol Al solubility was much higher
449 for TSP (14-28%) than PM_{2.5} (2-23%) at the summit of Mount Heng, southern China.

450 On the other hand, a few other studies (Baker et al., 2020; Hsieh et al., 2023; Sakata et al.,
451 2023; Yang et al., 2023) found that aerosol Al solubility was higher in fine particles than coarse
452 particles. For example, aerosol Al solubility was found to increase with the decrease in particle
453 size over the tropical eastern Atlantic (Baker et al., 2020), being ~10.31% for particles in the
454 size of 0.36-0.61 μm and 0.43-4.53% for particles above 0.61 μm . At Hiroshima, southern
455 Japan, aerosol Al solubility was reported to be $8.82\pm 6.48\%$ for fine particles ($<1.3 \mu\text{m}$), more
456 than two times larger than that ($3.25\pm 3.41\%$) for coarse particles ($>1.3 \mu\text{m}$) (Sakata et al., 2023).
457 Baker and Jickells (2006) suggested that this is because fine particles have larger surface-to-
458 volume ratios and thus facilitate Al dissolution via acid processing. Hsieh et al. (2023) found
459 aerosol Al solubility to be 38% for fine particles (0.57-1.0 μm) but only 0.37% for coarse
460 particles ($>7.3 \mu\text{m}$) over the East China Sea, and suggested that the observed size-dependence
461 could be explained by the enrichment of anthropogenic Al (which has higher solubility than
462 dust Al) in fine particles. However, aerosol Al originates predominantly from mineral dust,
463 with little contributions from anthropogenic sources (Taylor and McLennan, 1985; Mahowald
464 et al., 2018), and fractional solubility of anthropogenic Al was not necessarily higher than
465 mineral dust (Li et al., 2022).

466 As discussed above, there is not clear yet how and why aerosol Al solubility varies with
467 particle size. Such discrepancy is at least partly because different leaching protocols were used
468 in previous studies to extract dissolved aerosol Al and thereby Al solubility obtained in
469 different studies was not directly comparable (Meskhidze et al., 2019; Li et al., 2023; Li et al.,

470 2024). Furthermore, mechanistic insights can be obtained by laboratory experiments which
471 examine the size dependence of the solubility and dissolution kinetics of Al for mineral dust
472 particles under atmospherically relevant conditions.

473 **5. Conclusions and atmospheric implications**

474 Deposition of mineral dust aerosol is a major external source of several nutrient and toxic
475 elements for surface water in open oceans, and thus have large impacts on marine
476 biogeochemistry; however, previous studies which estimated dust deposition flux into the
477 oceans reveals large discrepancies. Aerosol Al solubility, which is a critical parameter in using
478 dissolved Al concentrations in surface seawater as a tracer to constrain dust deposition flux,
479 remains poorly understood. In this work, we investigated seasonal variations of aerosol Al
480 solubility for supermicron ($>1\ \mu\text{m}$) and submicron ($<1\ \mu\text{m}$) aerosol particles at Xi'an and
481 Qingdao, both located in northern China, in attempt to elucidate the processes and mechanisms
482 which govern the variation of aerosol Al solubility in the atmosphere.

483 At Xi'an, aerosol Al solubility was low in general for both supermicron and submicron
484 particles, showing no obvious variability in different seasons or under different weather
485 conditions. This implies that chemical processing did not substantially enhance aerosol Al
486 solubility at Xi'an, as it is an inland city close to major deserts in northwestern China and thus
487 the aging extent of mineral dust particles arriving at Xi'an was quite limited. Compared to
488 Xi'an, aerosol Al solubility was higher at Qingdao, a coastal city in northern China;
489 furthermore, Al solubility was higher in the other three seasons than in spring, and much higher
490 for haze- and especially fog-impacted days than dust days. This indicates that chemical
491 processing substantially increased aerosol Al solubility at Qingdao.

492 Aerosol Al solubility at Xi'an showed no significant correlation with relative abundance
493 of sulfate or nitrate, and did not vary apparently with RH; in contrast, Al solubility at Qingdao
494 was well correlated with relative abundance of sulfate and nitrate, and increased with RH. This
495 further supports that chemical processing had little impacts on aerosol Al solubility at Xi'an
496 (because the aging extent of mineral dust aerosol at Xi'an is very limited) but remarkably
497 increased aerosol Al solubility at Qingdao (because mineral dust particles transported to
498 Qingdao were substantially aged). Moreover, for both supermicron and submicron particles,
499 Al solubility at Qingdao was found to increase with aerosol acidity (in addition to RH),
500 underscoring the vital role of aerosol liquid water and acidity in enhancing Al dissolution via
501 chemical aging.

502 Our comprehensive investigation of aerosol Al solubility at two locations in Northern
503 China suggests that atmospheric chemical processing dictates aerosol Al solubility. As a result,
504 aerosol Al solubility is expected to spatially variable, depending on the extent of chemical
505 processing. For example, we found that aerosol Al solubility is higher at Qingdao than Xi'an
506 in general, and expect it to increase further as mineral dust aerosol is further transported
507 eastward to the Pacific. As a result, when leveraging dissolved Al concentrations in surface
508 seawater as a tracer to estimate deposition flux of mineral dust aerosol into open oceans,
509 considering the spatial distribution of aerosol Al solubility, instead of using a uniform value on
510 the global scale, can help us better constrain the oceanic deposition flux of mineral dust.

511

512 **Author contribution.**

513 **TZ:** Formal analysis, Investigation, Writing - Original Draft, Writing - Review & Editing;
514 **YC:** Formal analysis, Investigation, Writing - Original Draft; **HZ:** Investigation; **Lei Liu:**
515 Writing - Review & Editing; **CH:** Investigation; **ZF:** Investigation; **YZ:** Investigation; **FW:**
516 Resources; **Lan Luo:** Resources; **GZ:** Writing - Review & Editing; **XW:** Resources; **MT:**
517 Conceptualization, Formal analysis, Supervision; Writing - Original Draft, Writing - Review
518 & Editing.

519 **Competing interests.**

520 The authors declare that they have no conflict of interest.

521 **Acknowledgement.**

522 We would like to thank colleagues at Shandong University, Shaanxi University of Science
523 and Technology, and Institute of Earth Environment, Chinese Academy of Sciences for their
524 support during field measurements.

525 **Financial support.**

526 This work was sponsored by National Natural Science Foundation of China (42277088,
527 42407149 and 22361162668), Guangzhou Bureau of Science and Technology
528 (2024A04J6533), International Partnership Program of Chinese Academy of Sciences
529 (164GJHZ2024011FN), Guangdong Basic and Applied Basic Research Fund Committee
530 (2023A1515012010), and Guangdong Foundation for Program of Science and Technology
531 Research (2023B1212060049).

532

533

534 **References**

- 535 Aghnatiou, C., Losno, R., and Dulac, F.: A fine fraction of soil used as an aerosol analogue during the DUNE
536 experiment: sequential solubility in water, decreasing pH step-by-step, *Biogeosciences*, 11, 4627-4633,
537 <https://doi.org/10.5194/bg-11-4627-2014>, 2014.
- 538 Amram, K., and Ganor, J.: The combined effect of pH and temperature on smectite dissolution rate under acidic
539 conditions, *Geochim. Cosmochim. Acta*, 69, 2535-2546, <https://doi.org/10.1016/j.gca.2004.10.001>,
540 2005.
- 541 An, Z., Huang, R., Zhang, R., Tie, X., Li, G., Cao, J., Zhou, W., Shi, Z., Han, Y., Gu, Z., and Ji, Y.: Severe haze
542 in northern China: A synergy of anthropogenic emissions and atmospheric processes, *PNAS*, 116,
543 8657-8666, <https://doi.org/10.1073/pnas.1900125116>, 2019.
- 544 Anderson, R. F., Cheng, H., Edwards, R. L., Fleisher, M. Q., Hayes, C. T., Huang, K. F., Kadko, D., Lam, P. J.,
545 Landing, W. M., Lao, Y., Lu, Y., Measures, C. I., Moran, S. B., Morton, P. L., Ohnemus, D. C.,
546 Robinson, L. F., and Shelley, R. U.: How well can we quantify dust deposition to the ocean?, *Phil.
547 Trans. R. Soc. A*, 374: 20150285, <https://doi.org/10.1098/rsta.2015.0285>, 2016.
- 548 Baker, A. R., and Jickells, T. D.: Mineral particle size as a control on aerosol iron solubility, *Geophys. Res. Lett.*,
549 33, L17608, <https://doi.org/10.1029/2006gl026557>, 2006.
- 550 Baker, A. R., Jickells, T. D., Witt, M., and Linge, K. L.: Trends in the solubility of iron, aluminium, manganese
551 and phosphorus in aerosol collected over the Atlantic Ocean, *Mar. Chem.*, 98, 43-58,
552 <https://doi.org/10.1016/j.marchem.2005.06.004>, 2006.
- 553 Baker, A. R., and Croot, P. L.: Atmospheric and marine controls on aerosol iron solubility in seawater, *Mar.
554 Chem.*, 120, 4-13, <https://doi.org/10.1016/j.marchem.2008.09.003>, 2010.
- 555 Baker, A. R., Li, M., and Chance, R.: Trace Metal Fractional Solubility in Size - Segregated Aerosols From the
556 Tropical Eastern Atlantic Ocean, *Global Biogeochem. Cycles*, 34, e2019GB006510,
557 <https://doi.org/10.1029/2019gb006510>, 2020.
- 558 Benalabet, T., Lapid, G., and Torfstein, A.: Dissolved aluminium dynamics in response to dust storms, wet
559 deposition, and sediment resuspension in the Gulf of Aqaba, northern Red Sea, *Geochim. Cosmochim.
560 Acta*, 335, 137-154, <https://doi.org/10.1016/j.gca.2022.08.029>, 2022.
- 561 Bibi, I., Singh, B., and Silvester, E.: Dissolution of illite in saline-acidic solutions at 25°C, *Geochim.
562 Cosmochim. Acta*, 75, 3237-3249, <https://doi.org/10.1016/j.gca.2011.03.022>, 2011.
- 563 Bibi, I., Singh, B., and Silvester, E.: Dissolution kinetics of soil clays in sulfuric acid solutions: Ionic strength
564 and temperature effects, *Appl. Geochem.*, 51, 170-183,
565 <https://doi.org/10.1016/j.apgeochem.2014.10.004>, 2014.
- 566 Buck, C. S., Landing, W. M., Resing, J. A., and Measures, C. I.: The solubility and deposition of aerosol Fe and
567 other trace elements in the North Atlantic Ocean: Observations from the A16N CLIVAR/CO2 repeat
568 hydrography section, *Mar. Chem.*, 120, 57-70, <https://doi.org/10.1016/j.marchem.2008.08.003>, 2010.
- 569 Buck, C. S., Landing, W. M., and Resing, J.: Pacific Ocean aerosols: Deposition and solubility of iron,
570 aluminum, and other trace elements, *Mar. Chem.*, 157, 117-130,
571 <https://doi.org/10.1016/j.marchem.2013.09.005>, 2013.
- 572 Cao, J. J., and Cui, L.: Current Status, Characteristics and Causes of Particulate Air Pollution in the Fenwei
573 Plain, China: A Review, *J. Geophys. Res.-Atmos.*, 126, e2020JD034472,
574 <https://doi.org/10.1029/2020JD034472>, 2021.
- 575 Cappelli, C., Yokoyama, S., Cama, J., and Huertas, F. J.: Montmorillonite dissolution kinetics: Experimental and

576 reactive transport modeling interpretation, *Geochim. Cosmochim. Acta*, 227, 96-122,
577 <https://doi.org/10.1016/j.gca.2018.01.039>, 2018.

578 Chance, R., Jickells, T. D., and Baker, A. R.: Atmospheric trace metal concentrations, solubility and deposition
579 fluxes in remote marine air over the south-east Atlantic, *Mar. Chem.*, 177, 45-56,
580 <https://doi.org/10.1016/j.marchem.2015.06.028>, 2015.

581 Chen, Y., Wang, Z., Fang, Z., Huang, C., Xu, H., Zhang, H., Zhang, T., Wang, F., Luo, L., Shi, G., Wang, X., and
582 Tang, M.: Dominant Contribution of Non-dust Primary Emissions and Secondary Processes to
583 Dissolved Aerosol Iron, *Environ. Sci. Technol.*, 58, 17355-17363,
584 <https://doi.org/10.1021/acs.est.4c05816>, 2024.

585 Fang, Z., Dong, S., Huang, C., Jia, S., Wang, F., Liu, H., Meng, H., Luo, L., Chen, Y., Zhang, H., Li, R., Zhu, Y.,
586 and Tang, M.: On using an aerosol thermodynamic model to calculate aerosol acidity of coarse
587 particles, *J. Environ. Sci.*, 148, 46-56, <https://doi.org/10.1016/j.jes.2023.07.001>, 2025.

588 Fitzgerald, E., Ault, A. P., Zauscher, M. D., Mayol-Bracero, O. L., and Prather, K. A.: Comparison of the mixing
589 state of long-range transported Asian and African mineral dust, *Atmos. Environ.*, 115, 19-25,
590 <https://doi.org/10.1016/j.atmosenv.2015.04.031>, 2015.

591 Fountoukis, C., and Nenes, A.: ISORROPIA II: a computationally efficient thermodynamic equilibrium model
592 for K^+ - Ca^{2+} - Mg^{2+} - NH_4^+ - Na^+ - SO_4^{2-} - NO_3^- - Cl^- - H_2O aerosols, *Atmos. Chem. Phys.*, 7, 4639-4659,
593 <https://doi.org/10.5194/acp-7-4639-2007>, 2007.

594 Fu, H., Lin, J., Shang, G., Dong, W., Grassian, V. H., Carmichael, G. R., Li, Y., and Chen, J.: Solubility of Iron
595 from Combustion Source Particles in Acidic Media Linked to Iron Speciation, *Environ. Sci. Technol.*,
596 46, 11119-11127, <https://doi.org/10.1021/es302558m>, 2012.

597 Grand, M. M., Measures, C. I., Hattala, M., Hiscock, W. T., Buck, C. S., and Landing, W. M.: Dust deposition in
598 the eastern Indian Ocean: The ocean perspective from Antarctica to the Bay of Bengal, *Global
599 Biogeochem. Cycles*, 29, 357-374, <https://doi.org/10.1002/2014GB004898>, 2015.

600 Guo, L., Chen, Y., Wang, F., Meng, X., Xu, Z., and Zhuang, G.: Effects of Asian dust on the atmospheric input
601 of trace elements to the East China Sea, *Mar. Chem.*, 163, 19-27,
602 <https://doi.org/10.1016/j.marchem.2014.04.003>, 2014.

603 Han, Q., Moore, J. K., Zender, C., Measures, C., and Hydes, D.: Constraining oceanic dust deposition using
604 surface ocean dissolved Al, *Global Biogeochem. Cycles*, 22, GB2003,
605 <https://doi.org/10.1029/2007GB002975>, 2008.

606 Hsieh, C.-C., You, C.-F., and Ho, T.-Y.: The solubility and deposition flux of East Asian aerosol metals in the
607 East China Sea: The effects of aeolian transport processes, *Mar. Chem.*, 253, 104268,
608 <https://doi.org/10.1016/j.marchem.2023.104268>, 2023.

609 Hsu, S.-C., Wong, G. T. F., Gong, G.-C., Shiah, F.-K., Huang, Y.-T., Kao, S.-J., Tsai, F., Candice Lung, S.-C.,
610 Lin, F.-J., Lin, I. I., Hung, C.-C., and Tseng, C.-M.: Sources, solubility, and dry deposition of aerosol
611 trace elements over the East China Sea, *Mar. Chem.*, 120, 116-127,
612 <https://doi.org/10.1016/j.marchem.2008.10.003>, 2010.

613 Huneus, N., Schulz, M., Balkanski, Y., Griesfeller, J., Prospero, J., Kinne, S., Bauer, S., Boucher, O., Chin, M.,
614 Dentener, F., Diehl, T., Easter, R., Fillmore, D., Ghan, S., Ginoux, P., Grini, A., Horowitz, L., Koch, D.,
615 Krol, M. C., Landing, W., Liu, X., Mahowald, N., Miller, R., Morcrette, J. J., Myhre, G., Penner, J.,
616 Perlwitz, J., Stier, P., Takemura, T., and Zender, C. S.: Global dust model intercomparison in AeroCom
617 phase I, *Atmos. Chem. Phys.*, 11, 7781-7816, <https://doi.org/10.5194/acp-11-7781-2011>, 2011.

618 Ito, A., and Shi, Z.: Delivery of anthropogenic bioavailable iron from mineral dust and combustion aerosols to

619 the ocean, *Atmos. Chem. Phys.*, 16, 85-99, <https://doi.org/10.5194/acp-16-85-2016>, 2016.

620 Ito, A., Ye, Y., Baldo, C., and Shi, Z.: Ocean fertilization by pyrogenic aerosol iron, *npj Clim. Atmos. Sci.*, 4, 30,
621 <https://doi.org/10.1038/s41612-021-00185-8>, 2021.

622 Jeong, G. Y.: Mineralogy and geochemistry of Asian dust: dependence on migration path, fractionation, and
623 reactions with polluted air, *Atmos. Chem. Phys.*, 20, 7411-7428, [https://doi.org/10.5194/acp-20-7411-](https://doi.org/10.5194/acp-20-7411-2020)
624 [2020](https://doi.org/10.5194/acp-20-7411-2020), 2020.

625 Jiang, H.-B., Hutchins, D. A., Zhang, H.-R., Feng, Y.-Y., Zhang, R.-F., Sun, W.-W., Ma, W., Bai, Y., Wells, M.,
626 He, D., Jiao, N., Wang, Y., and Chai, F.: Complexities of regulating climate by promoting marine
627 primary production with ocean iron fertilization, *Earth Sci. Rev.*, 249, 104675,
628 <https://doi.org/10.1016/j.earscirev.2024.104675>, 2024.

629 Jickells, T. D., An, Z. S., Andersen, K. K., Baker, A. R., Bergametti, G., Brooks, N., Cao, J. J., Boyd, P. W.,
630 Duce, R. A., Hunter, K. A., Kawahata, H., Kubilay, N., laRoche, J., Liss, P. S., Mahowald, N.,
631 Prospero, J. M., Ridgwell, A. J., Tegen, I., and Torres, R.: Global Iron Connections Between Desert
632 Dust, Ocean Biogeochemistry, and Climate, *Science*, 308, 67-71,
633 <https://doi.org/10.1126/science.1105959>, 2005.

634 Jickells, T. D., Baker, A. R., and Chance, R.: Atmospheric transport of trace elements and nutrients to the
635 oceans, *Phil. Trans. R. Soc. A*, 374, 20150286, <https://doi.org/10.1098/rsta.2015.0286>, 2016.

636 Kok, J. F., Storelvmo, T., Karydis, V. A., Adebisi, A. A., Mahowald, N. M., Evan, A. T., He, C., and Leung, D.
637 M.: Mineral dust aerosol impacts on global climate and climate change, *Nat. Rev. Earth Environ.*, 4,
638 71-86, <https://doi.org/10.1038/s43017-022-00379-5>, 2023.

639 Li, R., Zhang, H., Wang, F., Ren, Y., Jia, S., Jiang, B., Jia, X., Tang, Y., and Tang, M.: Abundance and fractional
640 solubility of phosphorus and trace metals in combustion ash and desert dust: Implications for
641 bioavailability and reactivity, *Sci. Total Environ.*, 816, 151495,
642 <https://doi.org/10.1016/j.scitotenv.2021.151495>, 2022.

643 Li, R., Dong, S., Huang, C., Yu, F., Wang, F., Li, X., Zhang, H., Ren, Y., Guo, M., Chen, Q., Ge, B., and Tang,
644 M.: Evaluating the effects of contact time and leaching solution on measured solubilities of aerosol
645 trace metals, *Appl. Geochem.*, 148, 105551, <https://doi.org/10.1016/j.apgeochem.2022.105551>, 2023.

646 Li, R., Panda, P. P., Chen, Y., Zhu, Z., Wang, F., Zhu, Y., Meng, H., Ren, Y., Kumar, A., and Tang, M.: Aerosol
647 trace element solubility determined using ultrapure water batch leaching: an intercomparison study of
648 four different leaching protocols, *Atmos. Meas. Tech.*, 17, 3147-3156, [https://doi.org/10.5194/amt-17-](https://doi.org/10.5194/amt-17-3147-2024)
649 [3147-2024](https://doi.org/10.5194/amt-17-3147-2024), 2024.

650 Li, T., Wang, Y., Zhou, J., Wang, T., Ding, A., Nie, W., Xue, L., Wang, X., and Wang, W.: Evolution of trace
651 elements in the planetary boundary layer in southern China: Effects of dust storms and aerosol-cloud
652 interactions, *J. Geophys. Res.-Atmos.*, 122, 3492-3506, <https://doi.org/10.1002/2016JD025541>, 2017.

653 Li, W., Shao, L., Shi, Z., Chen, J., Yang, L., Yuan, Q., Yan, C., Zhang, X., Wang, Y., Sun, J., Zhang, Y., Shen, X.,
654 Wang, Z., and Wang, W.: Mixing state and hygroscopicity of dust and haze particles before leaving
655 Asian continent, *J. Geophys. Res.-Atmos.*, 119, 1044-1059, <https://doi.org/10.1002/2013JD021003>,
656 2014.

657 Liu, Y., Wu, Z., Wang, Y., Xiao, Y., Gu, F., Zheng, J., Tan, T., Shang, D., Wu, Y., Zeng, L., Hu, M., Bateman, A.
658 P., and Martin, S. T.: Submicrometer Particles Are in the Liquid State during Heavy Haze Episodes in
659 the Urban Atmosphere of Beijing, China, *Environ. Sci. Technol. Lett.*, 4, 427-432,
660 <https://doi.org/10.1021/acs.estlett.7b00352>, 2017.

661 López-García, P., Gelado-Caballero, M. D., Collado-Sánchez, C., and Hernández-Brito, J. J.: Solubility of

662 aerosol trace elements: Sources and deposition fluxes in the Canary Region, *Atmos. Environ.*, 148,
663 167-174, <https://doi.org/10.1016/j.atmosenv.2016.10.035>, 2017.

664 Mahowald, N.: Aerosol Indirect Effect on Biogeochemical Cycles and Climate, *Science*, 334, 794-796,
665 <https://doi.org/10.1126/science.1207374>, 2011.

666 Mahowald, N. M., Hamilton, D. S., Mackey, K. R. M., Moore, J. K., Baker, A. R., Scanza, R. A., and Zhang, Y.:
667 Aerosol trace metal leaching and impacts on marine microorganisms, *Nat. Commun.*, 9, 2614,
668 <https://doi.org/10.1038/s41467-018-04970-7>, 2018.

669 Measures, C. I., and Brown, E. T.: Estimating Dust Input to the Atlantic Ocean Using Surface Water Aluminium
670 Concentrations, in: *The Impact of Desert Dust Across the Mediterranean*, edited by: Guerzoni, S., and
671 Chester, R., Springer Netherlands, Dordrecht, 301-311, 1996.

672 Measures, C. I., and Vink, S.: On the use of dissolved aluminum in surface waters to estimate dust deposition to
673 the ocean, *Global Biogeochem. Cycles*, 14, 317-327, <https://doi.org/10.1029/1999GB001188>, 2000.

674 Measures, C. I., Sato, T., Vink, S., Howell, S., and Li, Y. H.: The fractional solubility of aluminium from mineral
675 aerosols collected in Hawaii and implications for atmospheric deposition of biogeochemically
676 important trace elements, *Mar. Chem.*, 120, 144-153, <https://doi.org/10.1016/j.marchem.2009.01.014>,
677 2010.

678 Meskhidze, N., Völker, C., Al-Abadleh, H. A., Barbeau, K., Bressac, M., Buck, C., Bundy, R. M., Croot, P.,
679 Feng, Y., Ito, A., Johansen, A. M., Landing, W. M., Mao, J., Myriokefalitakis, S., Ohnemus, D.,
680 Pasquier, B., and Ye, Y.: Perspective on identifying and characterizing the processes controlling iron
681 speciation and residence time at the atmosphere-ocean interface, *Mar. Chem.*, 217, 103704,
682 <https://doi.org/10.1016/j.marchem.2019.103704>, 2019.

683 Moore, C. M., Mills, M. M., Arrigo, K. R., Berman-Frank, I., Bopp, L., Boyd, P. W., Galbraith, E. D., Geider, R.
684 J., Guieu, C., Jaccard, S. L., Jickells, T. D., La Roche, J., Lenton, T. M., Mahowald, N. M., Marañón,
685 E., Marinov, I., Moore, J. K., Nakatsuka, T., Oeschies, A., Saito, M. A., Thingstad, T. F., Tsuda, A., and
686 Ulloa, O.: Processes and patterns of oceanic nutrient limitation, *Nature Geoscience*, 6, 701-710,
687 <https://doi.org/10.1038/ngeo1765>, 2013.

688 Pan, X., Uno, I., Wang, Z., Nishizawa, T., Sugimoto, N., Yamamoto, S., Kobayashi, H., Sun, Y., Fu, P., Tang, X.,
689 and Wang, Z.: Real-time observational evidence of changing Asian dust morphology with the mixing of
690 heavy anthropogenic pollution, *Sci. Rep.*, 7, 335, <https://doi.org/10.1038/s41598-017-00444-w>, 2017.

691 Paris, R., Desboeufs, K. V., Formenti, P., Nava, S., and Chou, C.: Chemical characterisation of iron in dust and
692 biomass burning aerosols during AMMA-SOP0/DABEX: implication for iron solubility, *Atmos. Chem.*
693 *Phys.*, 10, 4273-4282, <https://doi.org/10.5194/acp-10-4273-2010>, 2010.

694 Prospero, J. M., Ginoux, P., Torres, O., Nicholson, S. E., and Gill, T. E.: Environmental characterization of
695 global sources of atmospheric soil dust identified with the Nimbus 7 Total Ozone Mapping
696 Spectrometer (TOMS) absorbing aerosol product, *Rev. Geophys.*, 40, 2-1-2-31,
697 <https://doi.org/10.1029/2000RG000095>, 2002.

698 Riemer, N., Ault, A. P., West, M., Craig, R. L., and Curtis, J. H.: Aerosol Mixing State: Measurements,
699 Modeling, and Impacts, *Rev. Geophys.*, 57, 187-249, <https://doi.org/10.1029/2018RG000615>, 2019.

700 Sakata, K., Sakaguchi, A., Yamakawa, Y., Miyamoto, C., Kurisu, M., and Takahashi, Y.: Measurement report:
701 Stoichiometry of dissolved iron and aluminum as an indicator of the factors controlling the fractional
702 solubility of aerosol iron – results of the annual observations of size-fractionated aerosol particles in
703 Japan, *Atmos. Chem. Phys.*, 23, 9815-9836, <https://doi.org/10.5194/acp-23-9815-2023>, 2023.

704 Schroth, A. W., Crusius, J., Sholkovitz, E. R., and Bostick, B. C.: Iron solubility driven by speciation in dust

705 sources to the ocean, *Nature Geoscience*, 2, 337-340, <https://doi.org/10.1038/ngeo501>, 2009.

706 Schulz, M., Prospero, J. M., Baker, A. R., Dentener, F., Ickes, L., Liss, P. S., Mahowald, N. M., Nickovic, S.,
707 García-Pando, C. P., Rodríguez, S., Sarin, M., Tegen, I., and Duce, R. A.: Atmospheric Transport and
708 Deposition of Mineral Dust to the Ocean: Implications for Research Needs, *Environ. Sci. Technol.*, 46,
709 10390-10404, <https://doi.org/10.1021/es300073u>, 2012.

710 Sedwick, P. N., Sholkovitz, E. R., and Church, T. M.: Impact of anthropogenic combustion emissions on the
711 fractional solubility of aerosol iron: Evidence from the Sargasso Sea, *Geochem. Geophys. Geosyst.*, 8,
712 <https://doi.org/10.1029/2007GC001586>, 2007.

713 Shang, T., Kong, L., and Qi, J.: Metal elements in atmospheric aerosols during different pollution events in the
714 coastal region of the Yellow Sea: Concentration, solubility and deposition flux, *Mar. Pollut. Bull.*, 206,
715 116711, <https://doi.org/10.1016/j.marpolbul.2024.116711>, 2024.

716 Shelley, R. U., Landing, W. M., Ussher, S. J., Planquette, H., and Sarthou, G.: Regional trends in the fractional
717 solubility of Fe and other metals from North Atlantic aerosols (GEOTRACES cruises GA01 and
718 GA03) following a two-stage leach, *Biogeosciences*, 15, 2271-2288, <https://doi.org/10.5194/bg-15-2271-2018>, 2018.

720 Shelley, R. U., Baker, A. R., Thomas, M., and Murphy, S.: Aerosol trace element solubility and deposition fluxes
721 over the Mediterranean Sea and Black Sea basins, *Biogeosciences*, 22, 585-600,
722 <https://doi.org/10.5194/bg-22-585-2025>, 2025.

723 Shi, J., Guan, Y., Ito, A., Gao, H., Yao, X., Baker, A. R., and Zhang, D.: High Production of Soluble Iron
724 Promoted by Aerosol Acidification in Fog, *Geophys. Res. Lett.*, 47, e2019GL086124,
725 <https://doi.org/10.1029/2019GL086124>, 2020.

726 Shi, Z. B., Woodhouse, M. T., Carslaw, K. S., Krom, M. D., Mann, G. W., Baker, A. R., Savov, I., Fones, G. R.,
727 Brooks, B., Drake, N., Jickells, T. D., and Benning, L. G.: Minor effect of physical size sorting on iron
728 solubility of transported mineral dust, *Atmos. Chem. Phys.*, 11, 8459-8469, <https://doi.org/10.5194/acp-11-8459-2011>, 2011.

730 Sholkovitz, E. R., Sedwick, P. N., and Church, T. M.: Influence of anthropogenic combustion emissions on the
731 deposition of soluble aerosol iron to the ocean: Empirical estimates for island sites in the North
732 Atlantic, *Geochim. Cosmochim. Acta*, 73, 3981-4003, <https://doi.org/10.1016/j.gca.2009.04.029>, 2009.

733 Song, M., Jeong, R., Kim, D., Qiu, Y., Meng, X., Wu, Z., Zuend, A., Ha, Y., Kim, C., Kim, H., Gaikwad, S.,
734 Jang, K. S., Lee, J. Y., and Ahn, J.: Comparison of Phase States of PM(2.5) over Megacities, Seoul and
735 Beijing, and Their Implications on Particle Size Distribution, *Environ. Sci. Technol.*, 56, 17581-17590,
736 <https://doi.org/10.1021/acs.est.2c06377>, 2022.

737 Sullivan, R. C., Guazzotti, S. A., Sodeman, D. A., and Prather, K. A.: Direct observations of the atmospheric
738 processing of Asian mineral dust, *Atmos. Chem. Phys.*, 7, 1213-1236, <https://doi.org/10.5194/acp-7-1213-2007>, 2007.

740 Sun, J., Liu, L., Xu, L., Wang, Y., Wu, Z., Hu, M., Shi, Z., Li, Y., Zhang, X., Chen, J., and Li, W.: Key Role of
741 Nitrate in Phase Transitions of Urban Particles: Implications of Important Reactive Surfaces for
742 Secondary Aerosol Formation, *J. Geophys. Res.-Atmos.*, 123, 1234-1243,
743 <https://doi.org/10.1002/2017JD027264>, 2018.

744 Takahashi, Y., Higashi, M., Furukawa, T., and Mitsunobu, S.: Change of iron species and iron solubility in Asian
745 dust during the long-range transport from western China to Japan, *Atmos. Chem. Phys.*, 11, 11237-
746 11252, <https://doi.org/10.5194/acp-11-11237-2011>, 2011.

747 Tang, M., Cziczo, D. J., and Grassian, V. H.: Interactions of Water with Mineral Dust Aerosol: Water

748 Adsorption, Hygroscopicity, Cloud Condensation, and Ice Nucleation, *Chem. Rev.*, 116, 4205-4259,
749 <https://doi.org/10.1021/acs.chemrev.5b00529>, 2016.

750 Taylor, S. R., and McLennan, S. M.: The continental crust: Its composition and evolution, Blackwell Scientific
751 Publications, Oxford, 312 pp., 1985.

752 Trochkin, D., Iwasaka, Y., Matsuki, A., Yamada, M., Kim, Y.-S., Nagatani, T., Zhang, D., Shi, G.-Y., and Shen,
753 Z.: Mineral aerosol particles collected in Dunhuang, China, and their comparison with chemically
754 modified particles collected over Japan, *J. Geophys. Res.-Atmos.*, 108, 8642,
755 <https://doi.org/10.1029/2002JD003268>, 2003.

756 Virkkula, A., Teinilä, K., Hillamo, R., Kerminen, V. M., Saarikoski, S., Aurela, M., Viidanoja, J., Paatero, J.,
757 Koponen, I. K., and Kulmala, M.: Chemical composition of boundary layer aerosol over the Atlantic
758 Ocean and at an Antarctic site, *Atmos. Chem. Phys.*, 6, 3407-3421, [https://doi.org/10.5194/acp-6-3407-](https://doi.org/10.5194/acp-6-3407-2006)
759 [2006](https://doi.org/10.5194/acp-6-3407-2006), 2006.

760 Walters, W. W., and Hastings, M. G.: Collection of Ammonia for High Time-Resolved Nitrogen Isotopic
761 Characterization Utilizing an Acid-Coated Honeycomb Denuder, *Anal. Chem.*, 90, 8051-8057,
762 <https://doi.org/10.1021/acs.analchem.8b01007>, 2018.

763 Wang, G. H., Cheng, C. L., Huang, Y., Tao, J., Ren, Y. Q., Wu, F., Meng, J. J., Li, J. J., Cheng, Y. T., Cao, J. J.,
764 Liu, S. X., Zhang, T., Zhang, R., and Chen, Y. B.: Evolution of aerosol chemistry in Xi'an, inland
765 China, during the dust storm period of 2013 - Part 1: Sources, chemical forms and formation
766 mechanisms of nitrate and sulfate, *Atmos. Chem. Phys.*, 14, 11571-11585, [https://doi.org/10.5194/acp-](https://doi.org/10.5194/acp-14-11571-2014)
767 [14-11571-2014](https://doi.org/10.5194/acp-14-11571-2014), 2014.

768 Wang, S., Yan, Q., Zhang, R., Jiang, N., Yin, S., and Ye, H.: Size-fractionated particulate elements in an inland
769 city of China: Deposition flux in human respiratory, health risks, source apportionment, and dry
770 deposition, *Environmental Pollution*, 247, 515-523, <https://doi.org/10.1016/j.envpol.2019.01.051>,
771 2019.

772 Westberry, T. K., Behrenfeld, M. J., Shi, Y. R., Yu, H., Remer, L. A., and Bian, H.: Atmospheric nourishment of
773 global ocean ecosystems, *Science*, 380, 515-519, <https://doi.org/10.1126/science.abq5252>, 2023.

774 Wu, F., Zhang, D., Cao, J., Guo, X., Xia, Y., Zhang, T., Lu, H., and Cheng, Y.: Limited production of sulfate and
775 nitrate on front-associated dust storm particles moving from desert to distant populated areas in
776 northwestern China, *Atmos. Chem. Phys.*, 17, 14473-14484, [https://doi.org/10.5194/acp-17-14473-](https://doi.org/10.5194/acp-17-14473-2017)
777 [2017](https://doi.org/10.5194/acp-17-14473-2017), 2017.

778 Wuttig, K., Wagener, T., Bressac, M., Dammshäuser, A., Streu, P., Guieu, C., and Croot, P. L.: Impacts of dust
779 deposition on dissolved trace metal concentrations (Mn, Al and Fe) during a mesocosm experiment,
780 *Biogeosciences*, 10, 2583-2600, [10.5194/bg-10-2583-2013](https://doi.org/10.5194/bg-10-2583-2013), 2013.

781 Xu, H., and Weber, T.: Ocean Dust Deposition Rates Constrained in a Data-Assimilation Model of the Marine
782 Aluminum Cycle, *Global Biogeochem. Cycles*, 35, e2021GB007049,
783 <https://doi.org/10.1029/2021GB007049>, 2021.

784 Yang, J., Ma, L., He, X., Au, W. C., Miao, Y., Wang, W. X., and Nah, T.: Measurement report: Abundance and
785 fractional solubilities of aerosol metals in urban Hong Kong – insights into factors that control aerosol
786 metal dissolution in an urban site in South China, *Atmos. Chem. Phys.*, 23, 1403-1419,
787 <https://doi.org/10.5194/acp-23-1403-2023>, 2023.

788 Zhang, H., Li, R., Dong, S., Wang, F., Zhu, Y., Meng, H., Huang, C., Ren, Y., Wang, X., Hu, X., Li, T., Peng, C.,
789 Zhang, G., Xue, L., Wang, X., and Tang, M.: Abundance and Fractional Solubility of Aerosol Iron
790 During Winter at a Coastal City in Northern China: Similarities and Contrasts Between Fine and

791 Coarse Particles, *J. Geophys. Res.-Atmos.*, 127, e2021JD036070,
792 <https://doi.org/10.1029/2021JD036070>, 2022.

793 Zhang, H., Li, R., Huang, C., Li, X., Dong, S., Wang, F., Li, T., Chen, Y., Zhang, G., Ren, Y., Chen, Q., Huang,
794 R., Chen, S., Xue, T., Wang, X., and Tang, M.: Seasonal variation of aerosol iron solubility in coarse
795 and fine particles at an inland city in northwestern China, *Atmos. Chem. Phys.*, 23, 3543-3559,
796 <https://doi.org/10.5194/acp-23-3543-2023>, 2023.

797 Zhang, L., Kojima, T., and Zhang, D.: Origins and Aging of Calcium-rich Mineral Particles in Asian Dust
798 Arriving in Southwestern Japan: A Comparison of Slow- and Fast-moving Events, *Aerosol Sci. Eng.*,
799 <https://doi.org/10.1007/s41810-024-00275-z>, 2024.

800 Zhang, R., Jing, J., Tao, J., Hsu, S. C., Wang, G., Cao, J., Lee, C. S. L., Zhu, L., Chen, Z., Zhao, Y., and Shen,
801 Z.: Chemical characterization and source apportionment of PM_{2.5} in Beijing: seasonal perspective,
802 *Atmos. Chem. Phys.*, 13, 7053-7074, <https://doi.org/10.5194/acp-13-7053-2013>, 2013.

803 Zhang, X. Y., Gong, S. L., Shen, Z. X., Mei, F. M., Xi, X. X., Liu, L. C., Zhou, Z. J., Wang, D., Wang, Y. Q., and
804 Cheng, Y.: Characterization of soil dust aerosol in China and its transport and distribution during 2001
805 ACE-Asia: 1. Network observations, *J. Geophys. Res.-Atmos.*, 108, 4261,
806 <https://doi.org/10.1029/2002JD002632>, 2003.

807 Zhi, M., Wang, G., Xu, L., Li, K., Nie, W., Niu, H., Shao, L., Liu, Z., Yi, Z., Wang, Y., Shi, Z., Ito, A., Zhai, S.,
808 and Li, W.: How Acid Iron Dissolution in Aged Dust Particles Responds to the Buffering Capacity of
809 Carbonate Minerals during Asian Dust Storms, *Environ. Sci. Technol.*, 59, 6167-6178,
810 <https://doi.org/10.1021/acs.est.4c12370>, 2025.

811